Molecular organization in binary mixtures of derivatives of naphthalenebicarboxylic acid and naphthoylenebenzimidazole with a liquid crystal in two-dimensional layers II. Langmuir-Blodgett films

Andrzej Biadasz[a]; Tomasz Martyński[a]; Roland Stolarski[b]; Danuta Bauman[a]

[a] Faculty of Technical Physics, Poznań University of Technology, 60-965 Poznań, Poland [b] Institute of Polymer Technology and Dyes, Łódź University of Technology, 91-224 Łódź, Poland

PLEASE SCROLL DOWN FOR ARTICLE

Taylor & Francis
Taylor & Francis Group

Molecular organization in binary mixtures of derivatives of naphthalenebicarboxylic acid and naphthoylenebenzimidazole with a liquid crystal in two-dimensional layers II. Langmuir–Blodgett films

ANDRZEJ BIADASZ†, TOMASZ MARTYŃSKI†, ROLAND STOLARSKI‡ and DANUTA BAUMAN*†

†Faculty of Technical Physics, Poznań University of Technology, 60-965 Poznań, Poland
‡Institute of Polymer Technology and Dyes, Łódź University of Technology, 91-224 Łódź, Poland

Langmuir–Blodgett (LB) films of some dichroic dyes, namely derivatives of naphthalenebicarboxylic acid and derivatives of naphthoylenebenzimidazole, and of their mixtures with mesogens: 4-octyl-4′-cyanobiphenyl or 4-pentyl-4″-cyano-*p*-terphenyl were prepared. Absorption and fluorescence studies using unpolarized and linearly polarized light were carried out. Both absorption and fluorescence spectra indicated the formation of aggregates of dye molecules in monomolecular layers. Moreover, it was found that dye molecules are more tilted to the quartz surface in LB films than to the plane of the air–water interface in Langmuir films.

1. Introduction

The Langmuir–Blodgett (LB) technique enables us to position particular molecules or particles at precise distances from others in two-dimensional layers, the optical and electric properties of which can be easily manipulated [1–3]. These features make the LB technique unique and versatile in molecular electronics. Furthermore, spectroscopic and morphological studies of LB films provide valuable insight into the correlation between molecular organization and spectral properties.

The molecular organization in LB films inherently depends upon molecular states in spread monolayers on the water surface (Langmuir films) [1–4]. In the first part of this paper [5] we described the investigation of Langmuir films fabricated from some dichroic dyes, namely derivatives of naphthalenebicarboxylic acid and of naphthoylenebenzimidazole, and their binary mixtures with the mesogenic compounds 4-octyl-4′-cyanobiphenyl (8CB) and 4-pentyl-4″-cyano-*p*-terphenyl (5CT). We found that the dyes investigated, both pure and mixed with 8CB or 5CT, can form compressible homogeneous monolayers at an air–water interface. The molecular packing density, rigidity and stability of such monolayers depend strongly on the structure of dye and liquid crystal molecules and vary with the mixture composition. The dyes are highly miscible with 8CB, but immiscible or, at best, partially miscible with 5CT.

In this paper we describe the study of the above-mentioned dyes with 8CB or 5CT in LB films. It was our intention to determine the spectral characteristic of the dyes in two-dimensional films at the air–solid substrate interface and to determine the molecular organization and intermolecular interactions in such films.

2. Experimental

The dyes studied are shown in tables 1 and 2.

All the dyes were synthesized and chromatographically purified at the Institute of Polymer Technology and Dyes, Łódź University of Technology, Poland. The liquid crystal materials, 4-octyl-4′-cyanobiphenyl (8CB) and 4-pentyl-4″-cyano-*p*-terphenyl (5CT) were purchased from E. Merck (Germany) and were used without further purification.

In order to obtain Langmuir films, the compounds investigated were spread from chloroform (Uvasol, for spectroscopy, E. Merck) onto the deionized water subphase in a Minitrough 2 (KSV Instruments Ltd., Finland). Further experimental details about the preparation of the monolayer on the air–water interface are given elsewhere [5, 6].

Polished quartz plates ($35 \times 10 \times 1 \, \text{mm}^3$) were used as the solid substrates with a hydrophilic surface for LB film fabrication. The substrates were dipped and raised

*Corresponding author. Email: bauman@phys.put.poznan.pl

A. Biadasz et al.

Table 1. Derivatives of naphthalenebicarboxylic acid.
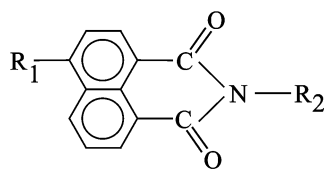
Dye code	R_1	R_2
1	—NH(CH$_2$)$_3$CH$_3$	—(CH$_2$)$_3$CH$_3$
2	—NH(CH$_2$)$_4$CH$_3$	—CH$_2$CH$_3$
3	—NH(CH$_2$)$_{11}$CH$_3$	—CH$_2$CH$_3$
4	—NH(CH$_2$)$_3$CH$_3$	—CH$_2$⟨phenyl⟩
5	—N⟨pyrrolidine⟩	—CH$_2$⟨phenyl⟩
6	—N(C$_8$H$_{17}$)$_2$	—⟨phenyl⟩—O—⟨phenyl⟩—CH$_3$

Table 2. Derivatives of naphthoylenebenzimidazole.

Dye code	R_1	R_2
7	—N(CH$_3$)$_2$	H
8	—N⟨pyrrolidine⟩	H
9	H	—NH(CH$_2$)$_2$CH$_3$
10	H	—NH—CH$_2$—⟨phenyl⟩

Figure 1. Geometry for the polarized absorption and fluorescence measurements. α is the incidence or emission angle. $\mathbf{E_P}$ and $\mathbf{E_S}$ are the electric vectors of incidence (absorption measurement) or emitted (fluorescence measurement) light polarized parallel and perpendicularly to the plane of incidence, respectively.

through the floating Langmuir film vertically at a speed of $5\,mm\,min^{-1}$. The Langmuir films were transferred onto the quartz plates at surface pressures below the collapse point, which corresponds to the formation of the compressed monolayer. The dipping stroke was 25 mm. The successful deposition of a film onto the quartz took place only on the up-stroke. The transfer ratio was estimated by calculating the ratio of the decrease in the subphase area to the area on the substrate coated by the layer. Values between 1.00 and 1.20 were obtained.

The absorption spectra of LB films were recorded in the UV-Vis region by means of a spectrophotometer CARY 400 (Varian, Australia); the fluorescence

measurements were carried out with a photon-counting spectrofluorimeter built in our laboratory and described in detail in [7]. The exciting light was the 436 nm line from a high pressure mercury lamp. Glan–Thomson polarizers and an angular sample holder were used in both absorption and fluorescence measurements using by polarized light. The measurements were performed in the geometry presented in figure 1.

3. Results and discussion

3.1. *Electronic absorption spectra*

Figures 2(a) and 2(b), respectively, show the long wavelength absorption spectra of pure dyes **2** and **10**, as examples, in LB films (curve 1) and, for comparison, dissolved in ethanol (curve 2). Table 3 lists the positions of the maximum and the half-bandwidths of the long wavelength absorption band for dyes **1–10** in ethanol. In figures 3(a) and 3(b) absorption spectra for pure dyes **2** and **9** (curve 1), pure liquid crystal (curve 5) and dye/liquid crystal mixtures at various molar fractions (MF) of the dye (curves 2–4) in LB films are presented. The positions of the maximum and half-bandwidths of the long wavelength absorption band for dyes **1–10**, pure and mixed with 8CB and 5CT, in LB films are given in tables 4 and 5, respectively.

The absorption spectra of pure **1–10** in the LB film reveal quite large spectral broadening in comparison with those in dilute solutions. The position of the maximum of the long 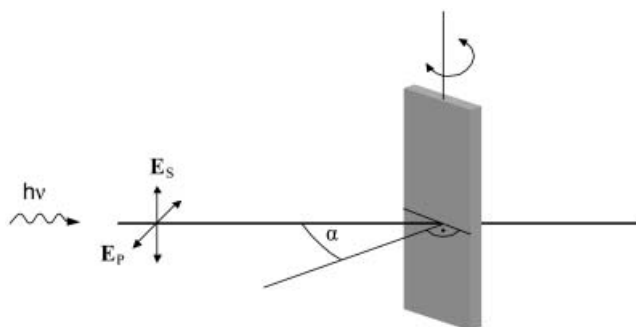wavelength absorption band of derivatives of naphthalenebicarboxylic acid does not change significantly, whereas in the case of derivatives
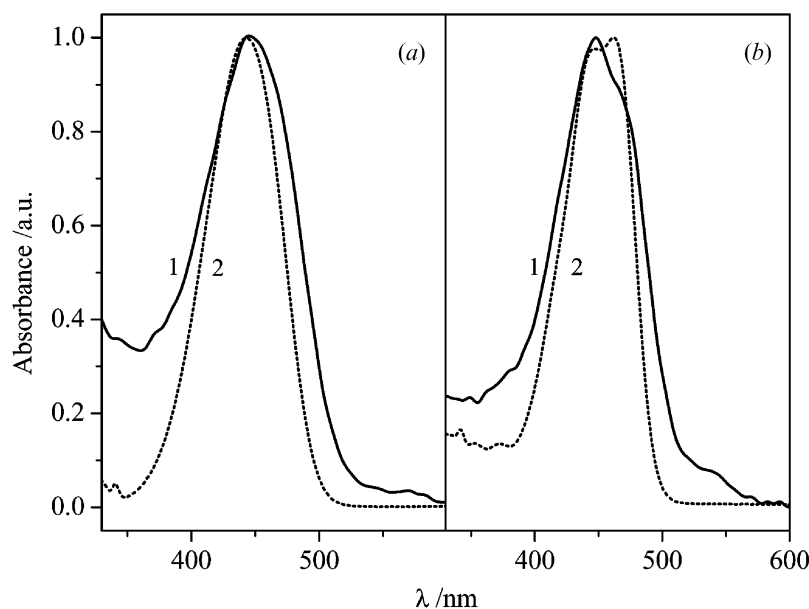

Figure 2. Normalized long wavelength absorption spectra of dyes **2** (a) and **10** (b) in LB film (1) and ethanol (2).

Table 3. Maximum position (λ_{max}) and half-band width (δ) of long wavelength absorption band of **1**–**10** in ethanol (MF$=2.5 \times 10^{-6}$).

Dye code	λ_{max}/nm $\Delta\lambda = \pm 1$ nm	δ/cm$^{-1}\Delta\delta = \pm 10$ cm^{-1}
1	446	3580
2	450	3520
3	447	3510
4	446	3560
5	446	3550
6	446	3580
7	468	4540
8	494	3970
9	452, 466	3120
10	441, 470	3260

of naphthoylenebenzimidazole, not only a bathochromic shift (up to 15 nm), but also some changes of the band shape, are observed. Note that in the case of dyes **1**–**6** the substituents to the rigid molecular core have almost no influence on the position and shape of the absorption band. However, for dyes **7**–**10** differences in the substituents have some effect on the wavelength of the maximum, as well as on the shape of the absorption band. As the concentration of the liquid crystals in mixed LB films rises the half-bandwidth of the absorption band of the dyes decreases, but no significant change in the positions of the maxima is observed. This implies that the bathochromic shift of the maximum of **1**–**10**, with respect to that in ethanol, may be due to the differing values of the refractive index and dielectric constant of ethanol and the mesogens.

The broadening of the absorption band of **1**–**10** and their mixtures with liquid crystals, at least at higher concentration, suggests aggregation between the dye molecules. Indeed neither an additional peak, nor a shoulder, which would suggest dimer creation in the ground state, is observed; but the absorbance of the band corresponding to the dye does not vary proportional to its concentration. For example, the content of **2** in 8CB in LB films, whose absorption spectra are shown in figure 2 (*a*), decreases by a factor of five. For comparison, the absorbance of the long wavelength band related to **2** decreases slightly less than four-fold. The changes of the band related to the liquid crystal (≈ 280 nm) are difficult to distinguish because of the overlapping of the absorption bands of the dye and the liquid crystal in this region of the spectrum. The ratios of the absorbance value of the pure dye to that of the dye mixed with the liquid crystal, for all the mixtures investigated in LB films, are listed in tables 6 and 7. It can be seen that the lack of the proportionality between the dye content in the mixture and the absorbance value occurs for all the dyes. This appears to confirm that some dye aggregation of **1**–**10** in LB films is already present in the ground electronic state. The changes of the absorbance are different for various dyes and various liquid crystals, which indicates the influence of the molecular structure of both components on the intermolecular interactions.

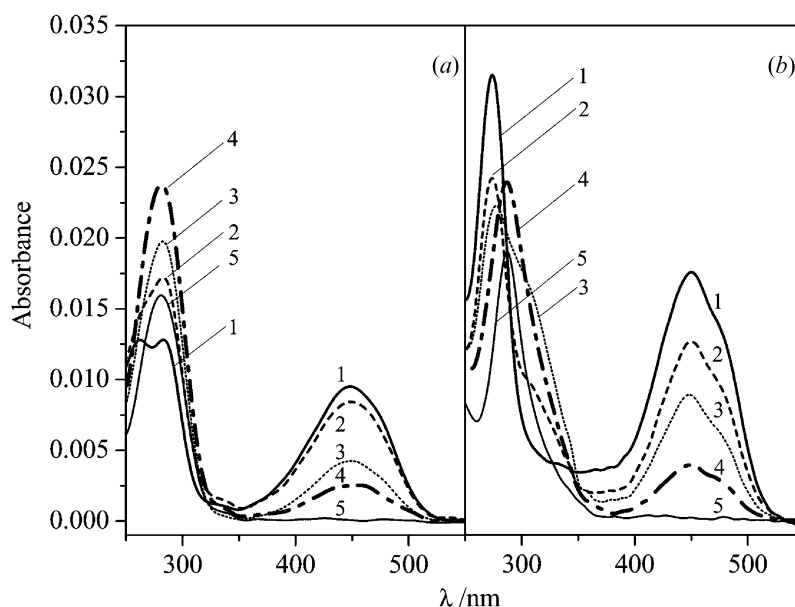Figure 3. Absorption spectra of pure dyes **2** (*a*) and **9** (*b*) (curve 1), pure 8CB (*a*) and 5CT (*b*) (curve 5) and of **2**/8CB (*a*) and **9**/5CT (*b*) mixtures at MF$=0.8$ (curve 2), MF$=0.5$ (curve 3) and MF$=0.2$ (curve 4) in LB films.

Table 4. Maximum position (λ_{max}) and half-bandwidth (δ) of long wavelength absorption band of **1**–**10** and their mixtures with 8CB in LB films at various molar fractions (MF).

	MF=1.0		MF=0.8		MF=0.5		MF=0.2	
Dye code	λ_{max}/nm $\Delta\lambda=\pm 1$ nm	δ/cm^{-1} $\Delta\delta=\pm 30$ cm^{-1}	λ_{max}/nm $\Delta\lambda=\pm 1$ nm	δ/cm^{-1} $\Delta\delta=\pm 30$ cm^{-1}	λ_{max}/nm $\Delta\lambda=\pm 1$ nm	δ/cm^{-1} $\Delta\delta=\pm 30$ cm^{-1}	λ_{max}/nm $\Delta\lambda=\pm 1$ nm	δ/cm^{-1} $\Delta\delta=\pm 30$ cm^{-1}
1	449	3970	448	3950	446	3820	449	3590
2	448	4060	449	4150	451	3750	452	3950
3	442	4160	440	4060	445	4210	445	3700
4	451	4150	448	4000	447	3860	446	3580
5	448	3830	446	3750	450	3630	—[a]	—[a]
6	449	3910	446	3960	444	4130	450	3900
7	483	5630	480	5770	487	5160	490	4220
8	498	4770	500	4480	502	4590	502	3860
9	450	4120	450	3900	450	3660	450	3530
10	447, 471	4060	447, 472	4390	448, 473	3590	449, 473	3780

[a]Absorption not measurable.

From exciton coupling theory [8, 9], it follows that if sufficiently strong electronic transitions exist, dipole–dipole interactions in molecular aggregates result in the splitting of the energy level of the excited state into two levels with higher and lower energy relative to the undisturbed excited state. The molar extinction coefficient of **1**–**10** is quite large, over 15 000 [10–12], thus the exciton coupling is most likely to occur in compressed monolayers.

In the molecular exciton model [8, 9] it is assumed that the intermolecular electron overlap of molecules in an aggregate is small and the molecules behave independently. Then, the perturbation theory yields the following energy values of the two excited molecular states, E' and E'', arising from the exciton splitting of the undisturbed localized transition N→K in both molecules [8]:

$$E' = E_{NK} - \Delta E_{NK}, \quad E'' = E_{NK} + \Delta E_{NK} \tag{1}$$

where E_{NK} is the excitation energy between the ground (N) and the excited (K) state of molecules and ΔE_{NK} is the dipole–dipole interaction energy between the two transition moments. $2\Delta E_{NK}$ is the exciton splitting energy, called Davydov splitting.

ΔE_{NK} can be calculated in the point-dipole approximation by:

$$\Delta E_{NK} = \frac{\mathbf{M}_i \cdot \mathbf{M}_j}{\mathbf{R}^3} - \frac{3(\mathbf{M}_i \cdot \mathbf{R})(\mathbf{M}_j \cdot \mathbf{R})}{\mathbf{R}^5} \tag{2}$$

where $\mathbf{M}_i$ and $\mathbf{M}_j$ are the electric dipole transition moments of molecules i and j, respectively, and $\mathbf{R}$ is the

Table 5. Maximum position (λ_{max}) and half-bandwidth (δ) of long wavelength absorption band of **1**–**10** and their mixture with 5CT in LB films at various molar fraction (MF).

	MF=1.0		MF=0.8		MF=0.5		MF=0.2	
Dye code	λ_{max}/nm $\Delta\lambda=\pm 1$ nm	δ/cm^{-1} $\Delta\delta=\pm 30$ cm^{-1}	λ_{max}/nm $\Delta\lambda=\pm 1$ nm	δ/cm^{-1} $\Delta\delta=\pm 30$ cm^{-1}	λ_{max}/nm $\Delta\lambda=\pm 1$ nm	δ/cm^{-1} $\Delta\delta=\pm 30$ cm^{-1}	λ_{max}/nm $\Delta\lambda=\pm 1$ nm	δ/cm^{-1} $\Delta\delta=\pm 30$ cm^{-1}
1	449	3970	446	3970	447	3800	—[a]	—[a]
2	448	4060	449	4240	451	3600	—[a]	—[a]
3	442	4160	439	4100	439	4070	439	3900
4	451	4150	451	4180	451	4040	452	3850
5	448	3830	448	4180	449	5440	—[a]	—[a]
6	449	3910	434	3900	432	3810	431	3360
7	483	5630	480	5360	484	5410	483	4900
8	498	4770	499	4770	501	4650	498	4230
9	450	4120	449	3840	448	3780	448	3600
10	447, 471	4060	445, 472	3890	445, 470	3990	445, 472	4040

[a]Absorption not measurable.

Table 6.   Ratios of the absorbance of the pure dye (A_D) to the absorbance of the dye mixed with 8CB (A_{mix}) in LB films at various molar fractions (MF).

Dye code	A_D/A_{mix}		
	MF=0.8	MF=0.5	MF=0.2
1	1.22	2.10	4.65
2	1.12	2.20	3.73
3	0.89	1.89	3.99
4	1.12	1.43	3.27
5	0.91	0.89	—
6	1.00	1.32	2.99
7	0.91	1.29	4.56
8	0.95	2.03	4.27
9	1.17	1.65	3.80
10	0.96	1.66	3.63

intermolecular distance vector connecting the centres of the molecules *i* and *j*.

Assuming the parallel configuration of dimer molecules of dyes **1**–**10**, the co-planar arrangement of the absorption transition moments can be considered. This leads to the exciton diagram shown in figure 4, and the exciton band splitting is given by the formula [8]:

$$\Delta E_{NK} = \frac{2|\mathbf{M}|^2}{\mathbf{R}^3} \left(1 - 3\cos^2\theta\right) \qquad (3)$$

where θ is the angle between the dipole transition moment of the molecule and $\mathbf{R}$. When $0° < \theta < 54.7°$, the exciton band is energetically located below the monomer band causing a red shift, and the aggregates created are called J-aggregates [13]. For $54.7° < \theta < 90°$, the exciton band is located energetically above the monomer band causing a blue shift, and corresponding aggregates are called H-aggregates [14]. When $\theta \approx 54.7°$,

Table 7.   Ratios of the absorbance of the pure dye (A_D) to the absorbance of the dye mixed with 5CT (A_{mix}) in LB films at various molar fractions (MF).

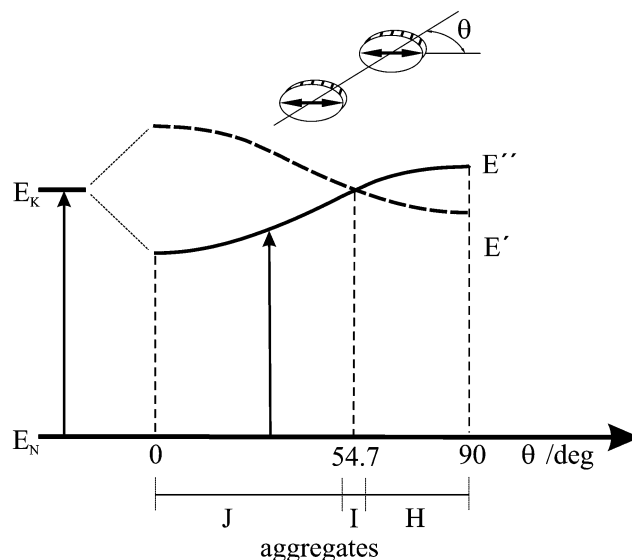| Dye code	A_D/A_{mix}		
	MF=0.8	MF=0.5	MF=0.2
1	1.11	1.91	—
2	1.09	1.99	—
3	0.87	1.12	2.64
4	1.03	1.47	4.61
5	0.89	0.86	—
6	0.58	0.88	1.66
7	0.58	0.94	4.47
8	0.93	1.01	2.55
9	1.35	1.93	4.28
10	3.28	1.37	3.28

Figure 4.   Exciton band energy diagram for a molecular dimer with co-planar arrangement of the transition moments inclined to the interconnecting axis by an angle θ.

no shift in the absorption spectrum is observed, and the aggregates are then called I-aggregates [15].

The distinct broadening of the absorption band of **1**–**10** in LB films (compared with that characteristic of monomers) with no shift of the absorption maximum position, implies that, in the case of derivatives of naphthalenebicarboxylic acid and of naphthoyleneben-zimidazole, we are dealing predominantly with I-aggregates in the ground state.

The measurements of the absorption using linearly polarized light for **1**–**10** were made in the geometry presented in figure 1. The spectra were run at incidence angles, α of $0°$, $30°$ and $60°$. On the basis of the polarized absorption spectra, the linear dichroism (LD) was determined. Following N'soukpoé-Kossi *et al.* [16] we defined LD by:

$$LD = \frac{A_P - A_S}{A_P + A_S} \qquad (4)$$

where A_P and A_S are the absorbance values at the band maximum for light polarized parallel and perpendicularly to the plane of incidence, respectively.

LD can be related to the angle of incidence α in the following way [16]:

$$LD_\alpha = \frac{2 - \tan^2\beta}{\tan^2\beta \frac{1 + \cos^2\alpha}{\sin^2\alpha} + 2} \qquad (5)$$

where β is the angle between the transition dipole moment vector and the normal to the plane of the LB film.
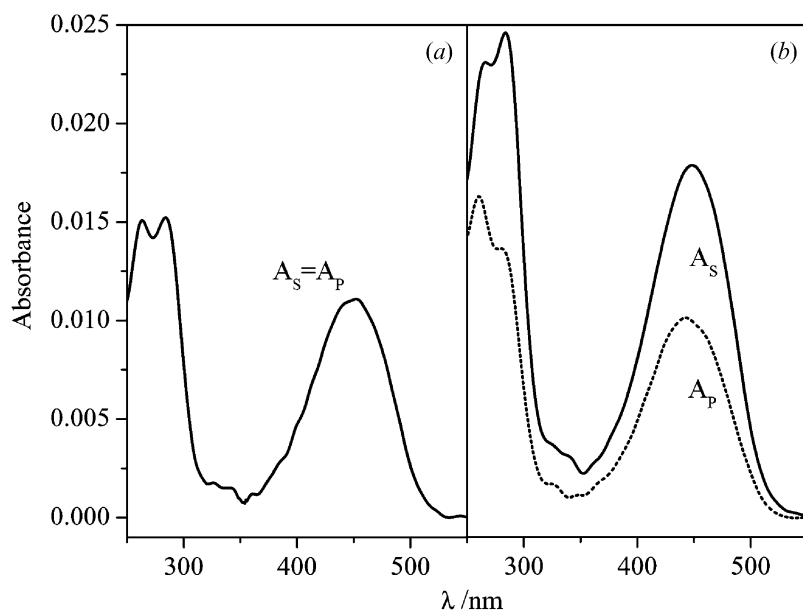
Figure 5. Polarized absorption spectra of dye **1** in LB films recorded at (*a*) $\alpha=0°$ and (*b*) $\alpha=60°$.

Equation (5) is valid if the molecules in the monolayer are distributed uniformly around the cone, with their transition moments tilted at an angle β to the normal. In this case the LD for $\alpha=0°$ should be equal to zero.

Figures 5 (*a*) and 6 (*a*), respectively, show the polarized absorption spectra recorded at $\alpha=0°$ for dyes **1** and **7**, as examples, in LB films. It can be seen that, for these dyes, the value of the linear dichroism for light incident perpendicularly to the quartz surface, $LD_{\alpha=0}$, is zero. This means that the movement of the quartz slide

during deposition did not disturb the homogeneity of the molecular alignment. For other compounds investigated we also obtained $LD_{\alpha=0}=0$. Thus, the angle β could be calculated from Equation (5) on the basis of the spectra measured at the angle $\alpha\neq0°$. The spectra of polarized absorption components recorded at $\alpha=60°$ for **1** and **7** are presented in figures 5 (*b*) and 6 (*b*), respectively.

In the case of dye/liquid crystal mixtures the values of $LD_{\alpha=0}$ were also always equal to zero, both for the long
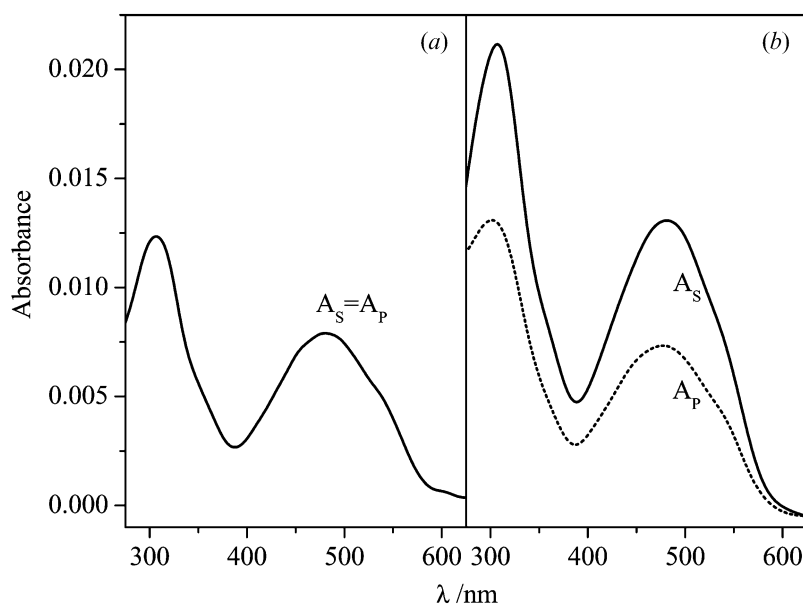

Figure 6. Polarized absorption spectra of dye **7** in LB films recorded at (*a*) $\alpha=0°$ and (*b*) $\alpha=60°$.
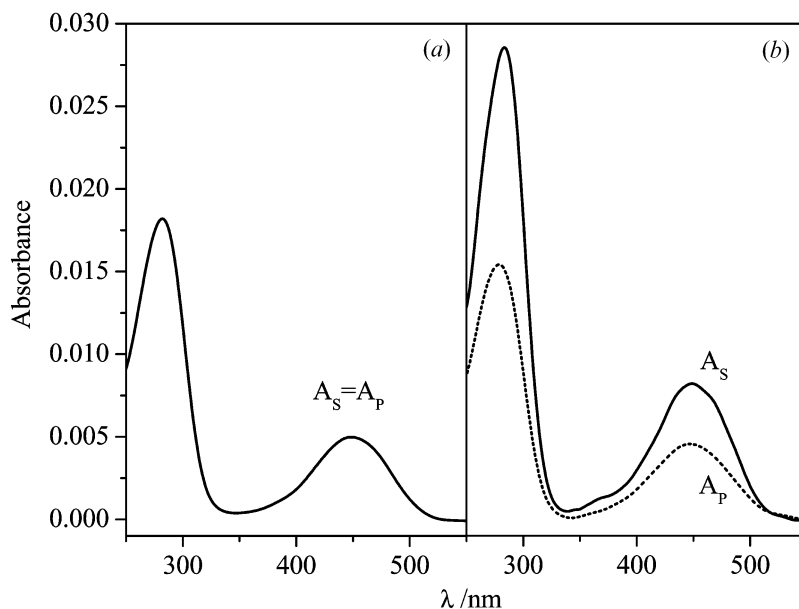
Figure 7.   Polarized absorption spectra of **2**/8CB mixture (MF=0.5) in LB films recorded at (*a*) α =0° and (*b*) α=60°.

wavelength and short wavelength bands, indicating a homogeneous distribution of both dye and liquid crystal molecules on the air–solid substrate interface. The characteristic polarized absorption spectra for **2**/8CB and **9**/5CT mixtures recorded at α=0° and 60° are shown in figures 7 and 8, respectively, and the values of β for all the dyes investigated in LB films are listed in tables 6 and 7. These are the mean values of the results obtained at the incidence angles α=30° and 60° for at least three independently prepared samples. LD_α values for these two incidence angles differ no more than 1.5°.

On the basis of the β angles listed in tables 8 and 9, we can obtain information about the orientation of the molecules of **1**–**10** with respect to the slide surface. A knowledge of the angle between the absorption oscillator and the molecular long axis of the dye is, however, necessary. The discussion of this problem for the dyes investigated has already been made [12, 17]. It follows
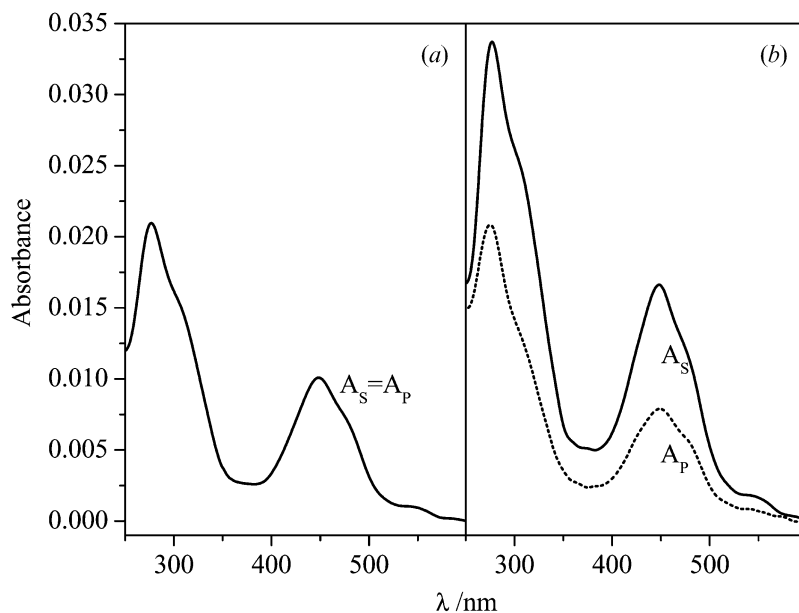
Figure 8.   Polarized absorption spectra of **9**/5CT mixture (MF=0.5) in LB films recorded at (*a*) α=0° and (*b*) α=60°.

Table 8. Values of the angle β between the transition dipole moment vector of the dyes and the normal to the plane in the LB film at various molar fractions (MF) in 8CB.

	β/deg $\Delta\beta = \pm 0.5$ deg			
Dye code	MF=1.0	MF=0.8	MF=0.5	MF=0.2
1	65.8	65.5	65.7	66.6
2	65.1	65.7	65.4	69.4
3	66.3	65.6	64.5	62.0
4	64.7	65.4	63.9	65.4
5[a]	—	—	—	—
6[a]	—	—	—	—
7	65.3	61.6	67.0	66.1
8	67.0	70.5	68.0	68.7
9	64.5	68.0	69.8	68.8
10	66.5	65.3	66.9	68.2

[a] The results for dyes **5** and **6** were unreliable.

that, to a first approximation, one can assume that the angle between the transition moment direction and the molecular long axis of **1–10** for the long wavelength absorption band, resulting from $\pi \to \pi^*$ transitions, is equal to zero. Thus, the angles β directly reflect the arrangement of dye molecules in the LB films. Comparing the values of β (tables 8 and 9) with those of the angle between the molecular long axis and the normal to the surface in Langmuir films, δ (tables 1–4 in [5]) for **1–10**, it can be seen that the rigid molecular cores of the dyes under investigation are significantly more tilted toward the solid surface in LB films than toward the water in Langmuir films. It is, therefore, clear that during the transfer of the monolayer from the air–water interface onto the solid substrate a molecular rearrangement takes place. This is illustrated schematically in figure 9. Similar observations have been made

Table 9. Values of the angle β between the transition dipole moment vector of the dyes and the normal to the plane of the LB film at various molar fractions (MF) in 5CT.

	β/deg $\Delta\beta = \pm 0.5$ deg			
Dye code	MF=1.0	MF=0.8	MF=0.5	MF=0.2
1	65.8	65.8	66.5	—
2	65.1	66.0	65.6	—
3	66.3	66.0	65.5	64.5
4	64.7	66.5	67.6	72.2
5[a]	—	—	—	—
6[a]	—	—	—	—
7	65.3	66.6	67.6	65.1
8	67.0	66.0	65.5	67.5
9	64.5	66.9	68.9	70.0
10	66.5	67.7	68.9	69.4

[a] The results for dyes **5** and **6** were unreliable.

previously for other compounds [7, 18–20]. The addition of the liquid crystal has virtually no influence on the arrangement of the dye molecules in LB films. Therefore, the behaviour of the absorbance of the band related to **1–10** for various mixture compositions, described previously, cannot be explained by the changes of molecular arrangement. It must instead be connected with some kind of dipole–dipole interaction in the ground state.

3.2. *Fluorescence spectra*

Figures 10(a) and 10(b) show, respectively, fluorescence spectra of pure dyes **2** and **10** in LB films (curve 1) and for comparison, dissolved in ethanol (curve 2). Table 10 shows the positions of the maximum and half-bandwidths of the fluorescence band for dyes **1–10** in ethanol. In figures 11(a) and 11(b) the normalized fluorescence spectra for pure dyes **2** and **9** (curve 1) and dye/liquid crystal mixtures at various MF of the dye (curves 2–4) in LB films are shown. The positions of the maximum and half-bandwidths of the fluorescence band for dyes **1–10**, pure and mixed with 8CB and 5CT in LB films, are given in tables 11 and 12, respectively.

The emission spectra of pure **1–10** in LB films are significantly different from the solution spectra. Not only is a broadening of the fluorescence band observed, but also there is a strong red shift of the maximum position. For derivatives of naphthalenebicarboxylic acid this shift is about 30 nm, whereas for derivatives of naphthoylenebenzimidazole a shift of up to 108 nm was found. Both the broadening of the fluorescence band, strong red shift and the lack of the appropriate band in the absorption spectrum are typical for the formation of excited dimers (excimers) [21]. Since the excimers (which originate from an interaction of neighbouring molecules after one is excited) do not exist in the ground state, it is clear that they cannot be seen in the absorption spectrum. Previously, we had found that LB films formed of 3,4,9,10-tetra(n-alkoxycarbonyl)perylenes, are characterized by an orange fluorescence with one peak about 550 nm (red-shifted 50–60 nm, depending on the alkyl chain length, with respect to the solution peak) and the loss of the vibrational fine structure [7, 20, 22–24], and ascribed these spectral change in the emission spectrum with respect to those of the solution to the formation of excimers. Similarly, Benning *et al.* [25, 26] have reported that crystals of pure perylene, pyrene and triphenylene compounds exhibit fluorescence spectra typical for excimers. In [26] results of the study of the emission spectra dependence on concentration for unsubstituted pyrene in ethanol are given; they show that at MF of 2.5×10^{-4} both the monomer and excimer
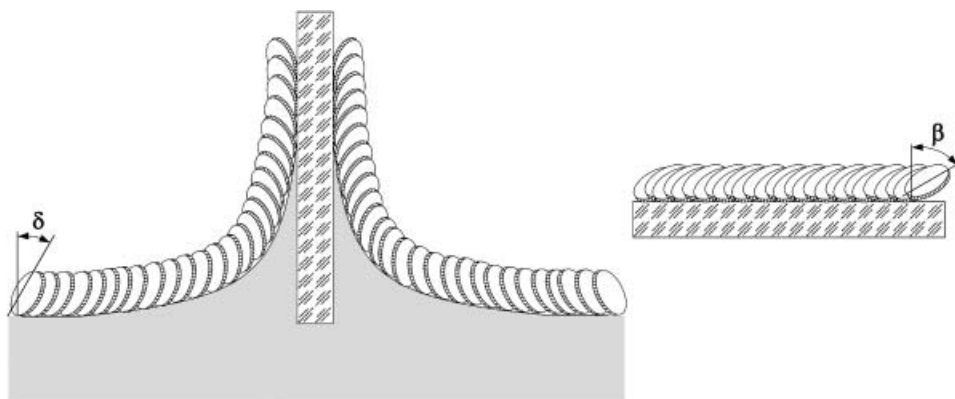
Figure 9.   Schematic representation of the change of the arrangement of **1**–**10** molecules during transfer from the air–water interface to the air–solid substrate interface.
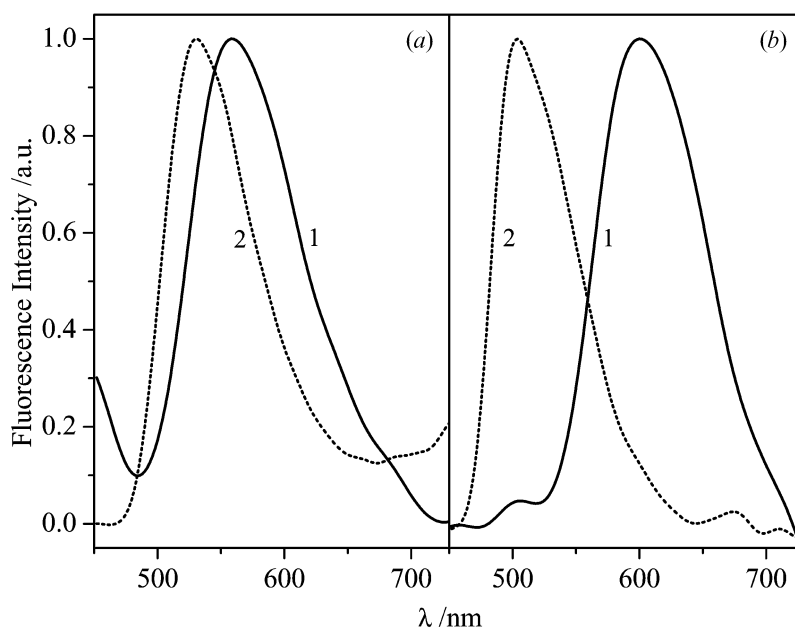

Figure 10.   Fluorescence spectra of dyes **2** (*a*) and **10** (*b*) in LB film (curve 1) and in ethanol (curve 2).

bands appear in the fluorescence spectra. However, in the fluorescence spectra of other dyes investigated in [26] excimer bands are absent up to a relatively high concentration of $MF=5.0 \times 10^{-4}$. Similar results for several perylene-like dyes have been described [12, 27, 28]. Naphthalene derivatives of bicarboxylic acid and derivatives of naphthoylenebenzimidazole were investigated in some liquid crystals up to $MF \approx 10^{-3}$ [10–12]. However, no excimer bands in the fluorescence spectra were found, which means that also in these cases, the excimer cannot be created below a threshold concentration.

In [24] the creation of excited dimers in LB films of 3,4,9,10-tetra(*n*-alkoxycarbonyl)perylenes mixed with

Table 10.   Maximum position (λ_{max}) and half-bandwidth (δ) of the fluorescence band of **1**–**10** in ethanol ($MF=2.5 \times 10^{-6}$).

Dye code	λ_{max}/nm $\Delta\lambda=\pm 1\,nm$	δ/cm^{-1} $\Delta\delta=\pm 20\,cm^{-1}$
1	534	2880
2	531	2830
3	532	2830
4	534	2830
5[a]	—	—
6	535	2970
7	618	2830
8	620	2530
9	508	2220
10	504	2680

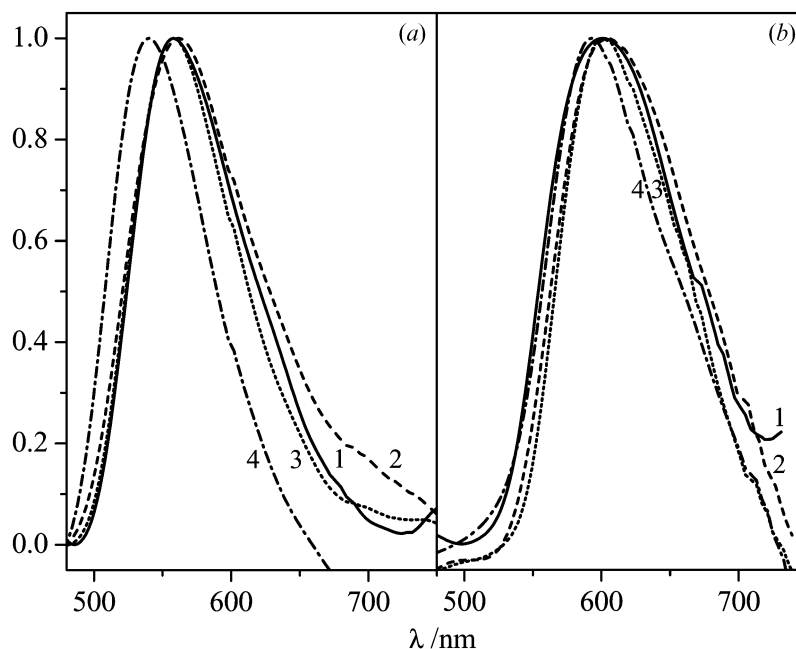[a]Dye **5** does not fluoresce in ethanol.

Figure 11.   Fluorescence spectra of dyes **2** (*a*) and **9** (*b*) (curve 1) and of **2**/8CB (*a*) and **9**/5CT (*b*) mixtures at MF=0.8 (curve 2), MF=0.5 (curve 3), MF=0.2 (curve 4), respectively, in LB films.

8CB at a dye concentration of $MF \geqslant 1.5 \times 10^{-2}$ was reported. Looking at the spectra presented in figure 11 as well as the data given in tables 11 and 12, and comparing these with the results for the dyes in ethanol (figure 10 and table 10), it can be seen that the derivatives of naphthalenebicarboxylic acid can form, at most, a small fraction of dimers in the excited state, but not below a dye concentration of MF=0.5. However, derivatives of naphthoylenebenzimidazole are able to form excimers at MF=0.2, or at even lower concentration. LB films with the dye concentration below MF=0.2 were not fabricated because their

fluorescence is not measurable. Therefore, in order to establish which concentration of dyes **9** and **10** is sufficient to give the excimer emission, these dyes must be studied at lower concentration using another technique, for example in 'sandwich' cells of $\approx 10\,\mu\text{m}$ in thickness, as used for 3,4,9,10-tetra(*n*-alkoxycarbonyl)perylenes in [24].

The difference in the red shift of the fluorescence maximum, as well as in the concentration at which excimer formation is observed, for dyes **1**–**6** and for dyes **7**–**10** in LB films, can be explained in terms of various degrees of overlap of the aromatic cores of molecules in

Table 11.   Maximum position ($\lambda_{\max}$) and half-bandwidth (δ) of the fluorescence band of **1**–**10** and their mixtures with 8CB in LB films at various molar fractions (MF).

Dye code	MF=1.0		MF=0.8		MF=0.5		MF=0.2	
	$\lambda_{\max}$/nm $\Delta\lambda=\pm 1\,\text{nm}$	δ/cm^{-1} $\Delta\delta=\pm 50\,\text{cm}^{-1}$	$\lambda_{\max}$/nm $\Delta\lambda=\pm 1\,\text{nm}$	δ/cm^{-1} $\Delta\delta=\pm 50\,\text{cm}^{-1}$	$\lambda_{\max}$/nm $\Delta\lambda=\pm 1\,\text{nm}$	δ/cm^{-1} $\Delta\delta=\pm 50\,\text{cm}^{-1}$	$\lambda_{\max}$/nm $\Delta\lambda=\pm 1\,\text{nm}$	δ/cm^{-1} $\Delta\delta=\pm 50\,\text{cm}^{-1}$
1	563	3110	558	3380	552	3010	534	2880
2	559	2880	558	3060	556	2740	539	2930
3	557	3200	554	3380	553	3110	542	3060
4	563	3550	565	3340	549	3230	548	3200
5[a]	—	—	—	—	—	—	—	—
6	554	3250	547	3110	548	3290	548	3020
7[a]	—	—	—	—	—	—	—	—
8[a]	—	—	—	—	—	—	—	—
9	601	2980	600	3020	602	2880	589	3110
10	601	2560	593	2790	591	2650	579	2880

[a]Dyes **5**, **7** and **8** do not fluoresce in 8CB.

Table 12. Maximum position (λ_{max}) and half-bandwidth (δ) of the fluorescence band of **1**–**10** and their mixtures with 5CT in LB films at various molar fractions (MF).

Dye code	MF=1.0		MF=0.8		MF=0.5		MF=0.2	
	λ_{max}/nm $\Delta\lambda=\pm 1$ nm	δ/cm^{-1} $\Delta\delta=\pm 50$ cm^{-1}	λ_{max}/nm $\Delta\lambda=\pm 1$ nm	δ/cm^{-1} $\Delta\delta=\pm 50$ cm^{-1}	λ_{max}/nm $\Delta\lambda=\pm 1$ nm	δ/cm^{-1} $\Delta\delta=\pm 50$ cm^{-1}	λ_{max}/nm $\Delta\lambda=\pm 1$ nm	δ/cm^{-1} $\Delta\delta=\pm 50$ cm^{-1}
1	563	3110	559	3660	548	3520	525	3340
2	559	2880	562	2880	548	3520	545	3440
3	557	3200	552	3610	553	3110	546	3200
4	563	3550	565	3380	564	3520	540	3520
5[a]	—	—	—	—	—	—	—	—
6	554	3250	544	3110	544	3060	542	3250
7[a]	—	—	—	—	—	—	—	—
8[a]	—	—	—	—	—	—	—	—
9	601	2980	603	3110	589	2510	593	2970
10	601	2560	603	2930	601	2930	588	2880

[a]Dyes **5**, **7** and **8** do not fluorescence in 5CT.

the monolayer at the quartz surface. It is possible that, because derivatives of naphthoylenebenzimidazole have only one terminal substituent, these dye molecules can overlap more than those of naphthalene derivatives of bicarboxylic acid which have two, sometimes long and bulky, terminal substituents. Such observations lead us to conclude that substitution with bulky lateral or terminal groups hinders the formation of dimers, and excimer formation is possible only at very high concentrations.

For LB films of pure **1**–**10** and of their mixtures with 8CB or 5CT the polarized components of the fluorescence spectra were also recorded. For excitation natural light was used. The results of the measurements revealed that the intensities of the components of the polarized fluorescence spectra for LB films, formed both of pure dye and dye/liquid crystal mixture, differ in very similar way as do the absorbances of the appropriate film. This indicates that the aggregates created in the excited state do not change the molecular organization at the air–solid substrate interface.

4. Conclusions

Six derivatives of naphthalenebicarboxylic acid (**1**–**6**) and four derivatives of naphthoylenebenzimidazole (**7**–**10**), together with their binary mixtures with mesogens 8CB and 5CT have been investigated as Langmuir–Blodgett films.

The molecules of **1**–**10** align with a significantly greater tilt angle with the normal to the solid surface, than with the normal to the air–water interface. This angle is virtually unchanged as mesogen concentration is raised. These results indicate that, during transfer of the monolayer from the water to the quartz slide, in the films formed both of pure dyes and of their binary

mixtures with liquid crystals, a rearrangement of the molecular packing takes place.

The shape and band positions of the absorption and emission spectra of **1**–**10**, pure and mixed with liquid crystals, suggest a tendency for aggregate formation between the dye molecules already in the ground electronic state. However, only excimers are revealed in the fluorescence spectrum of the LB films.

Acknowledgements

References

[1] G. Roberts. *Langmuir-Blodgett Films*. Plenum Press, New York (1990).
[2] A. Ulman. *An Introduction to Ultrathin Organic Films - from Langmuir-Blodgett to Self-Assembly*. Academic Press, New York (1991).
[3] M.C. Petty. *Langmuir-Blodgett Films - An Introduction*. Cambridge University Press (1996).
[4] G.L. Gaines. *Insoluble Monolayers at Liquid-Gas Interface*. Interscience, New York (1996).
[5] A. Biadasz, T. Martyński, R. Stolarski, D. Bauman. *Liq. Cryst.*, **31**, 1639 (2004).
[6] A. Biadasz, R. Hertmanowski, T. Martyński, K. Inglot, D. Bauman. *Dyes. Pigm.*, **56**, 209 (2003).
[7] R. Hertmanowski, Ł. Chudziński, T. Martyński, P. Stempniewicz, E. Wolarz, D. Bauman. *Liq. Cryst.*, **31**, 791 (2004).
[8] M. Kasha, H.R. Rawls, M. Ashraf El-Bayoumi. *Pure appl. Chem.*, **11**, 371 (1965).
[9] A.S. Davydov. *Theory of Molecular Excitons*. McGraw-Hill, New York (1962).
[10] T. Martyński, E. Mykowska, R. Stolarski, D. Bauman. *Dyes Pigm.*, **25**, 115 (1994).

[11] E. Mykowska, K. Jaźwińska, W. Grupa, D. Bauman. *Proc. SPIE*, **3318**, 378 (1998).

[12] E. Mykowska. PhD thesis, Poznań University of Technology, Poland (2000).

[13] G. Scheibe. *Angew. Chem.*, **50**, 51 (1937).

[14] G. Scheibe. *Angew. Chem.*, **49**, 563 (1936).

[15] A. Miyata, D. Heard, Y. Unuma, Y. Higashigaki. *Thin solid Films*, **210/211**, 175 (1992).

[16] Ch.N. N'soukpoé-Kossi, J. Sielewiesiuk, R.M. Leblanc, R.A. Bone, J.T. Landrum. *Biochim. Biophys.*, **940**, 255 (1988).

[17] E. Mykowska, K. Fiksiński, D. Bauman. *Proc. SPIE*, **4147**, 316 (2000).

[18] E. Johnson, R. Aroca, Y. Nagao. *J. phys. Chem.*, **95**, 8840 (1991).

[19] T. Martyński, A. Biadasz, D. Bauman. *Liq. Cryst.*, **29**, 281 (2002).

[20] R. Hertmanowski, T. Martyński, D. Bauman. *J. mol. Struct.*, **741**, 201 (2005).

[21] B. Stevens, M.I. Ban. *Trans. Faraday Soc.*, **60**, 1515 (1964).

[22] T. Martyński, R. Hertmanowski, D. Bauman. *Liq. Cryst.*, **28**, 445 (2001).

[23] R. Hertmanowski, A. Biadasz, T. Martyński, D. Bauman. *J. mol. Struct.*, **646**, 25 (2003).

[24] R. Hertmanowski, E. Chrzumnicka, T. Martyński, D. Bauman, *J. Lumin.* (submitted).

[25] S.A. Benning, H.-S. Kitzerow, H. Bock, M.-F. Achard. *Liq. Cryst.*, **27**, 901 (2000).

[26] S.A. Benning, T. Hassheider, S. Keuker-Baumann, H. Bock, F. Della Sala, T. Frauenheim, H.-S. Kitzerow. *Liq. Cryst.*, **28**, 1105 (2001).

[27] R. Stolarski, K. Fiksiński. *Dyes Pigm.*, **24**, 295 (1994).

[28] E. Mykowska, D. Bauman. *Z. Naturforsch.*, **51a**, 843 (1996).